We are IntechOpen,
the world's leading publisher of
Open Access books
Built by scientists, for scientists

4,800
Open access books available

122,000
International authors and editors

135M
Downloads

Our authors are among the

154
Countries delivered to

TOP 1%
most cited scientists

12.2%
Contributors from top 500 universities

CLARIVATE ANALYTICS
BOOK CITATION INDEX
INDEXED

WEB OF SCIENCE™

Selection of our books indexed in the Book Citation Index
in Web of Science™ Core Collection (BKCI)

Interested in publishing with us?
Contact book.department@intechopen.com

Chapter

The Use of Electrical Measurements of Wind Turbine Generators for Drive Train Condition Monitoring

Estefania Artigao, Andrés Honrubia-Escribano,
Sergio Martín-Martínez and Emilio Gómez-Lázaro

Abstract

More modern and larger wind turbine (WT) generators are under continuous development. These exhibit more faults than smaller ones, which becomes critical offshore. Under this framework, operation and maintenance (O&M) is the key to improve reliability and availability of WTs, where condition-based maintenance (CBM) is currently seen as the preferred approach by the early detection and diagnosis of critical faults for WTs. The induction generator is one of the biggest contributors to failure rates and downtime of WTs, together with the gearbox and the drive train. In the present chapter, current signature analysis (CSA) will be introduced as a means for fault detection of WTs. CSA is a cost-effective and nonintrusive technique that can monitor both mechanical and electrical faults within the induction generator, as well as bearing- and gearbox-related faults. Different test cases of in-service wind turbine generators will be used to illustrate its usefulness.

Keywords: condition monitoring, current signature analysis, DFIG, wind turbine, operation and maintenance, predictive maintenance, drive train

1. Introduction

Wind energy is currently the most mature, cost competitive and cost-efficient source of renewable energy. This has been proven through the levelized cost of electricity (LCOE), which is a very common measure to define the cost of any sort of electricity generation. The historical evolution of onshore and offshore wind LCOE is shown in **Figure 1**. As can be seen, the LCOE has continuously decreased during the past few years both for onshore and offshore wind power generation. Offshore wind has experienced a bigger drop than onshore, although it still shows a significantly higher LCOE.

With over 590 GW of wind power installed globally, the market intelligence of the Global Wind Energy Council (GWEC) expects over a 55 GW per year global increment of new installations (combining both offshore and onshore wind) until 2023 [1]. In the present scenario, China leads the onshore sector, followed by the
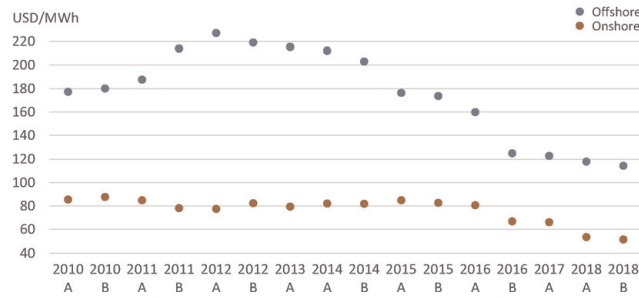
Figure 1.
Evolution of the LCOE for global onshore and offshore wind energy generation from 2010 to 2018.
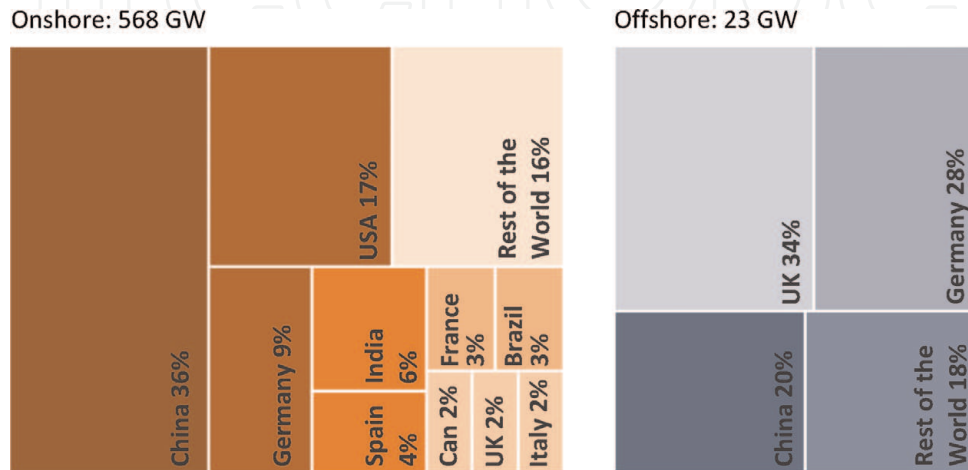

Figure 2.
Distribution of cumulative installed onshore and offshore wind energy capacity.

USA, Germany, India and Spain. The offshore sector is led by the UK, followed by Germany and China. The distribution of the top 10 countries with onshore wind power installed and the top 3 for offshore installations can be seen in **Figure 2**.

1.1 Reliability and availability

New sophisticated multi-MW wind turbines are constantly being developed [2–4], both for onshore and offshore applications [5]. Such rapid growth entails significant challenges that need attention from researchers and the industry [6]. In fact, more failures have been observed in large wind turbines than the small ones [7–9]. Current availability figures for onshore and offshore wind farms are found to be 97 and 85%, respectively [10, 11]. Accessibility issues and higher uncertainty are the reasons for the lower availability of offshore than the onshore.

Understanding which components are the most critical of a WT is the key to develop specific condition monitoring (CM) systems that will enhance O&M of wind farms, thus reliability and availability of WTs. To this end, this section presents the results published in the main failure rate and downtime surveys conducted in Europe, the USA and China. The major characteristics of these studies are summarised in **Table 1**, and the failure rate and downtime results presented in **Figure 3**.

As can be seen in **Figure 3**, both the electric and the control systems show the largest percentages for failure rates across the different studies (up to 32 and 42%, respectively) while hub and blades and gearbox for downtime (up to 38 and 56%, respectively). Medium percentages of failure rates and downtime are obtained for the generator, pitch and hydraulic systems. The braking system and drive train

Survey	Year	Location	WT number	WT capacity	On-/offshore
Acronym	Published			[MW]	
AWE [12]	2016	Europe	2270(av)	1–3	Onshore
CWEA [13]	2016	China	—	—	—
CARR [14]	2015	Europe	350	2–4	Offshore
B&W [15]	2014	UK	—	2.3	Onshore
CREW [16]	2013	USA	800–900	1.3–1.4	—
EZ [17]	2012	Netherlands	36	3	Offshore
RELI [18]	2011	Europe	350	>0.8	Onshore
VTT [19]	2010	Finland	72	0.2–2.3	Onshore
LWK [8]	2008	Germany	158–643	0.2–2	Onshore
WSDK [20]	2007	Denmark	851–2345	0.1–2.5	Onshore
WSD [20]	2007	Germany	1295–4285	0.1–2.5	Onshore
SW [7]	2007	Sweden	624(av)	0.5–1.5	Onshore
WMEP [9]	2006	Germany	>1500	—	Onshore

Table 1.
Characteristics of the main wind turbine reliability and availability surveys conducted in Europe, the USA and China.

present low failure rates but medium-to-high downtime. The sensors and structure categories present low values for both failure rates and downtime. Without considering the *others* category, the main contributors to failure rates across the different studies are hub & blades, electric, control and pitch systems. Similarly for the downtime, these are the gearbox, generator, mechanical brake and electric system assemblies.

If the main contributors both to failure rates and downtime are considered, then the control system, gearbox, electric system, generator and hub and blades could be considered the most critical components of wind turbines. Thus, special attention should be given to these components with regard to condition monitoring and O&M.

1.2 Operations and maintenance

One of the main leading costs of the wind farm's total expenditure belongs to O&M activities [12], representing between 25 and 35% for onshore and offshore wind farms, respectively, of their lifetime costs [21–23]. It is thus clear that reducing O&M costs would be beneficial for wind farm owners and operators.

Maintenance strategies can be typically classified as [21, 24] time-based (TBM), failure-based (FBM) and condition-based. TBM is formed by preventive tasks, also referred to as scheduled maintenance, and it is carried out regardless of the health state of the WT. FBM involves corrective actions, only performed after a critical failure has taken place, thus usually causing long downtime periods. CBM, on the other hand, is a predictive type of maintenance. CBM takes place only when there is a need but before a critical failure occurs, with the consequent saving in resources and downtime, thus achieving the optimum strategy [25, 26]. The different maintenance strategies are illustrated in **Figure 4**. Traditionally, a combination of TBM and FBM has been the preferred option among wind farm operators [17]. Lately, however, the trends are shifting towards CBM, which is performed through appropriate condition

monitoring, recognised by [27, 28] as the key for optimised reliability and availability of wind turbines while achieving cost reduction in O&M [29, 30].
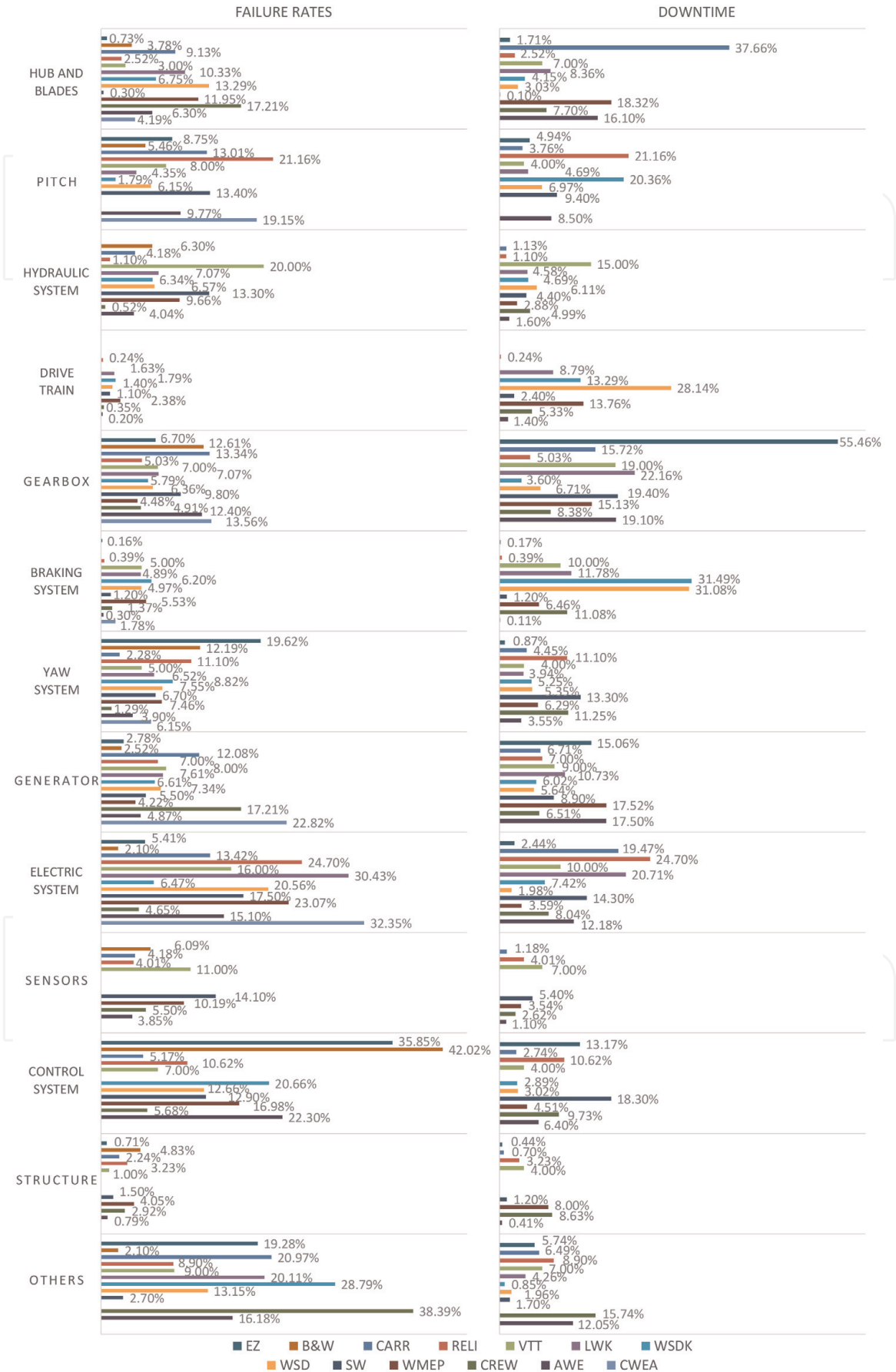

Figure 3.
Failure rates and downtime of several wind turbine reliability and availability studies spread in Europe, the USA and China.
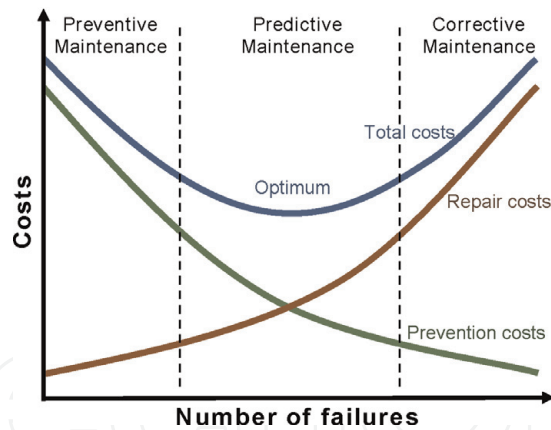
Figure 4.
Maintenance strategies.

1.3 Condition monitoring

CM consists of analysing different types of signals (such as temperature, vibrations, electrical measurements, etc.) with the aim of assessing the health of the component under study [24] towards calculating its remaining useful life (RUL) [31]. In this context, the implementation of CM systems must enable early-stage fault detection, so that CBM can be implemented, thus significantly reducing or even eliminating unscheduled (or unplanned) maintenance costs [32, 33]. Many CM and fault diagnosis reviews have been published in the last 15 years that include the latest CM methods [34, 35]. These can be classified per WT subsystem [36, 37] and differentiated between structural [38], mechanical [39], power electronics and control systems [40] or electrical parts [41–43].

Current commercial CM systems mainly target the WT drive train (particularly the gearbox) and are based on vibrations and oil analysis. The first ones to appear, and therefore the most common, were based on oil analysis. These systems, in addition to providing information on the status of the oil, are also capable to inform about the gears. They detect ferrous and non-ferrous particles, where the presence of ferrous particles is indicative of gear wear, while the presence of non-ferrous particles indicates oil degradation. Soon, a lot of research emerged based on vibration analysis, targeting the gearbox and bearings in the drive train. This type of analysis was adapted from other industries with rotating machinery. The latest commercial CM systems to appear were based on SCADA data. There are a large number of scientific publications utilising different parameters acquired by the SCADA system able to provide information of several components of the WT [44, 45]. Less common CM systems are based on acoustic emissions, strain gauges, thermographic analysis, etc.

On the other hand, with a non-negligible number of world-wide wind farms reaching the end of their expected 20-year lifetime [46], the field of lifetime extension (LTE) of wind turbines is gaining attention, where CM will also play a key role [47]. Different approaches are found for LTE of WTs such as practical inspections, field data analyses or analytical simulations. The authors in [48], for example, have identified data-driven approaches as the most cost-effective with large number of WTs.

1.4 Motivation

Data collection and analysis is not straightforward. There are many different techniques for signal processing and feature extraction, and, to date, no agreement

has been established on which CM system is the most appropriate for specific components or assemblies. Furthermore, most of the techniques and methods developed for CM of WTs have only been applied on laboratory benches. In fact, with regard to the generator, despite being one of the most critical components in a WT, no commercial CM system has yet been developed that can provide exhaustive information about its health status.

The goal of the present chapter is to present a CM method based on electrical measurements that can detect different generator faults and has been implemented on in-service operating WTs. CM methods based on electrical measurements can be performed using current, voltage, instantaneous power and flux analyses [49]. Of these, stator current spectral analysis (Current Signature Analysis, CSA) is recognised as the preferred option [50–52], thus chosen for this book chapter.

2. The method: current signature analysis

CSA is a nonintrusive method capable of identifying electrical and mechanical faults in a cost-effective manner [53–55]. It is based on the principle that different faults have different effects on the current spectra. It can be implemented on doubly-fed induction generators (DFIGs), which are the most common technology on variable speed WTs.

As reported in [56], bearing-related faults are the most common in WT generators, representing 59% of the total share, followed by stator faults with 28% and then rotor faults with 9% (the remaining 4% assigned to 'others'). These faults produce excessive heating, flux unbalance, voltages and/or phase current unbalance, decreased average torque, etc., thus negatively affecting the generator's efficiency [57]. Fault frequency components related to such faults are well known and have been demonstrated in different industries in different kinds of induction machines, including a few specific cases in WTs very recently [58–60]. The formulae to obtain the above-mentioned fault frequency components are presented in the following sub-sections.

2.1 Broken rotor bars, f_{BRB}

Broken rotor bars produce an asymmetry in the rotor electric and magnetic fields. As a result, frequency components appear in the stator current that generate speed fluctuation interacting with the supply frequency [61]. Fault frequency components in the presence of broken rotor bars can be calculated as [61–63]

$$f_{BRB} = f_s \pm 2sf_s \tag{1}$$

with f_s the supply frequency and s the slip.

It must be noted that certain degree of asymmetry will always be present in any induction machine (e.g. introduced in manufacturing); thus, the only presence of the components described in Eq. (1) may not indicate such fault. In order to differentiate between fault and no fault, the authors in [63–65] have identified the minimum difference between the amplitudes of such frequency components and the supply frequency that must be found.

Frequency components given by Eq. (1) appear near the supply frequency and overlap with different types of faults. For these reasons, different frequency

components have been developed by different authors that facilitate the identification of broken rotor bars, given by [66–68]

$$f_{BRB} = f_s \left[\kappa \left(\frac{1-s}{p} \right) \pm s \right] \tag{2}$$

with κ the harmonic index ($\kappa = 1, 2, 3, \ldots$) and p the number of pole pairs. Based on typical winding configurations, the authors in [52, 69] stated the relation $\kappa/p = 1, 5, 7, \ldots$.

2.2 Stator winding, f_{SW}

Stator winding faults normally develop from inter-turn short circuits [68, 70], where a negative magnetomotive force appears in the windings. As a result, the air-gap flux changes, thus inducing harmonic frequencies in the stator current. Fault frequency components related to stator winding fault are given by [68, 70, 71]

$$f_{SW} = f_s \left[\kappa \left(\frac{1-s}{p} \right) \pm n \right] \tag{3}$$

with $n = 1, 3, 5, \ldots$.

2.3 Bearing faults, f_{BE}

The mechanical displacement that takes place in the case of radial movement between rotor and stator originated with defective bearings results in frequency components in the stator current given by [50, 72]

$$f_{BE} = |f_s \pm \kappa f_{o,i}| \tag{4}$$

with $f_{o,i}$ referring to bearing outer and inner race fault, respectively, calculated as [52, 73, 74]

$$f_o = 0.4 N_b \frac{f_s(1-s)}{p} \tag{5}$$

$$f_i = 0.6 N_b \frac{f_s(1-s)}{p} \tag{6}$$

with N_b the number of bearing balls. These equations are simplifications valid for 8–12 ball bearings.

2.4 Gearbox faults, f_{GBX}

Gearbox damage can be of different nature, originating from a gearbox bearing, shaft, gear or pinion or a combination of them [53]. Therefore, different frequency components associated with a faulty gearbox can appear in the current spectrum. The authors in [75] identified frequency components related to damaged teeth, scoring and debris as

$$f_{GBX} = f_s \left(1 \pm \frac{\kappa}{G_r p} \right) \tag{7}$$

with G_r the gearbox ratio.

The most typical gearbox faults, however, are those related to shaft and gear faults [53, 76–80], calculated as Eqs. (8) and (9), respectively:

$$f^i_{FShaft} = f_s \pm \kappa f^i_{Shaft} \tag{8}$$

$$f^j_{FMesh} = f_s \pm \kappa f^j_{Mesh} \tag{9}$$

with f^i_{Shaft} the gearbox shaft rotating frequencies (with $i = 1, 2, 3 \dots$) and f^i_{Mesh} the gear mesh frequency (with $j = 1, 2, 3, \dots, i-1$).

2.5 Eccentricity, f_{ECC}

There are two main groups of fault frequency components associated to eccentricity faults [81]: high- and low-frequency components (HF and LF, respectively). HF components are calculated as [69]

$$f_{ECC,HF} = f_s \left[\pm \nu + (\kappa R \pm n_d) \frac{1-s}{p} \right] \tag{10}$$

with R the number of rotor slots, n_d the eccentricity order ($n_d = 0$ for static eccentricity and $n_d = 1, 2, 3, \dots$ for dynamic eccentricity) and ν the order of stator time harmonics ($\nu = 1, 3, 5, 7, \dots$).

Load torque oscillations and load variations do not affect these HF components as much as they affect LF components [81], and they can also separate the spectral components of air-gap eccentricity from broken rotor bars. However, it is necessary to know specific information of the induction machine under study [69].

LF components, on the other hand, appear near the supply frequency, and its magnitude increases in the case of mixed eccentricity. They can be calculated as [69]

$$f_{ECC,LF} = f_s \pm \kappa f_s \frac{1-s}{p} \tag{11}$$

2.6 Rotor asymmetry, f_{RFS}

Rotor mechanical asymmetries such as broken rotor bars, faulty end rings, etc. give rise to new frequency components in the stator current spectra [82–84] that can be calculated as

$$f_{RFS} = f_s (1 \pm 2\kappa s) \tag{12}$$

2.7 Rotor unbalance, f_{RU}

The authors in [85, 86] present a comprehensive analysis of the origins of rotor winding or brush gear unbalance faults, developing their associated analytical expressions. In their study, they identify separately health- and fault-related frequency components, calculated as Eqs. (13) and (14), respectively:

$$f_{HRU} = f_s |6\kappa(1-s) \pm l| \tag{13}$$

$$f_{FRU} = f_s \left| \frac{\kappa}{p}(1-s) \pm l \right| \tag{14}$$

with κ the harmonic constant for air-gap field space ($\kappa = 1, 2, 3, \ldots$) and l the supply time harmonic one ($l = \pm 1$).

2.8 Summary of fault-related frequencies and discussion

A summary of all fault-related frequency components is provided in **Table 2**.

The fault frequency components associated to the most common faults and their possible root causes have been presented. As can be seen, certain defects might produce other defects with the same effect on the current spectra. That is the case for the change in the air-gap flux caused by a fault in the stator winding (given by Eq. (3)), resulting in air-gap eccentricity (given by Eq. (11)), i.e. substituting Eq. (3) with $n = 1$ gives Eq. (11).

In the same way, stator winding impedances produce asymmetries that cause a resultant backward rotating field, thus affecting the rotor currents [73]; this is to say that faults originating in the stator will influence the rotor and vice versa. In fact, deriving from Eq. (3), the same components are obtained than those given by Eq. (14) with $l = 1$.

Further to fault-related frequency components, a number of frequency components that are non-fault related will appear in the stator current spectra of a healthy machine. That would be the case for the stator carrier frequency (i.e. the frequency

Fault	Formula	Eq. label	Constants
Broken rotor bar	$f_{BRB} = f_s \pm 2sf_s$	(1)	$\frac{\kappa}{p} = 1, 5, 7$
	$f_{BRB} = f_s \left[\kappa \left(\frac{1-s}{p} \right) \pm s \right]$	(2)	
Stator winding	$f_{SW} = f_s \left[\kappa \left(\frac{1-s}{p} \right) \pm n \right]$	(3)	$\kappa = 1, 2, 3$
			$n = 1, 3, 5$
Bearing damage	$f_{BE} = |f_s \pm \kappa f_{o,i}|$	(4)	$\kappa = 1, 2, 3$
	$f_o = 0.4 N_b \frac{f_s(1-s)}{p}$	(5)	
	$f_i = 0.6 N_b \frac{f_s(1-s)}{p}$	(6)	
Gearbox damage	$f_{GBX} = f_s \pm \kappa \left[\frac{f_s}{G_r p} \right]$	(7)	$\kappa = 1, 2, 3$
	$f^i_{FShaft} = f_s \pm \kappa f^i_{Shaft}$	(8)	
	$f^j_{FMesh} = f_s \pm \kappa f^j_{Mesh}$	(9)	
Air-gap eccentricity	$f_{ECC,HF} = f_s \left[\pm \nu + (\kappa R \pm n_d) \frac{1-s}{p} \right]$	(10)	$n_d = 0, 1, 2, 3$
			$\nu = 1, 3, 5, 7$
	$f_{ECC,LF} = f_s \left(1 \pm \kappa \frac{1-s}{p} \right)$	(11)	$\kappa = 1, 2, 3$
Rotor asymmetry	$f_{RFS} = f_s(1 \pm 2\kappa s)$	(12)	$\kappa = 1, 2, 3$
Rotor unbalance	$f_{HRU} = f_s |6\kappa(1-s) \pm l|$	(13)	$\kappa = 1, 2, 3$
	$f_{FRU} = f_s \left| \frac{\kappa}{p}(1-s) \pm l \right|$	(14)	$l = 1, 2, 3$

Table 2.
CSA formulae.
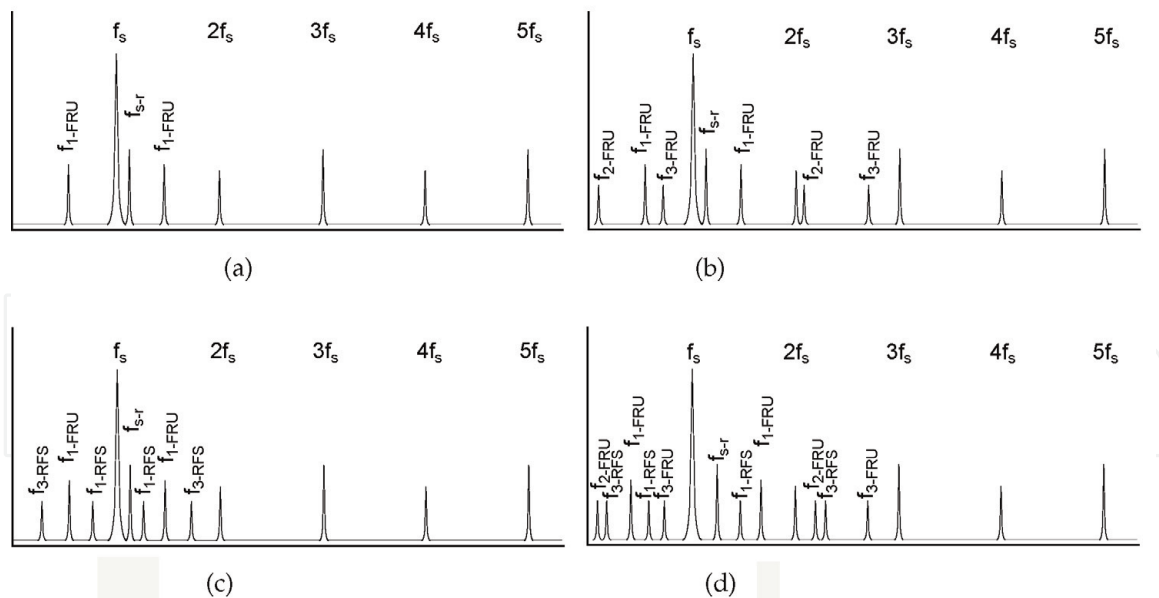
Figure 5.
Spectrum patterns of DFIG under healthy conditions and different fault conditions. (a) Healthy, (b) Rotor Electrical Unbalance, (c) Rotor Mechanical Unbalance, and (d) Rotor Winding Fault.

of the grid, f_s) and its odd and even harmonics ($2f_s, 3f_s, 4f_s, 5f_s \ldots$), which are normally present in the spectrum but are not indicative of fault. Another component that will be present in the case of a DFIG, and is not a fault indicator, is that corresponding to the difference between the stator carrier frequency (f_s) and the rotor carrier frequency (f_{rotor}) [58, 59]. This component will appear to the right of f_s when the DFIG operates at a super-synchronous speed (with negative slip). Contrarily, it will appear to the left of f_s at sub-synchronous speed (positive slip). Finally, as previously mentioned, frequency components given by Eq. (13) are not indicators of fault either.

All this highlights the fact that stator current spectra interpretation is not straightforward. Furthermore, fault frequency components are dependent on the rotational speed; thus the potential fault frequency components must be calculated for each operating condition. In order to exemplify in a schematic way typical CSA patterns, some are depicted in **Figure 5**, including that of a healthy DFIG spectra.

3. Case studies

This section presents the diagnosis of three different in-service WTs equipped with DFIGs using CSA. The WTs were located in different sites, thus belonging to different wind farms. Their rated power, number of pole pairs and generator technology vary from one another, as well as the monitoring period and sampling parameters. **Table 3** summarises the rated power (in kW), the monitoring period

	DFIG1	DFIG2	DFIG3
Nominal power [kW]	850	1500	1500
Monitoring period [months]	8	17	1
Sampling frequency [kHz]	1.5	1.5	12
Sampling time [s]	5.4	5.4	10.9

Table 3.
Main characteristics of the three databases used for the analysis.
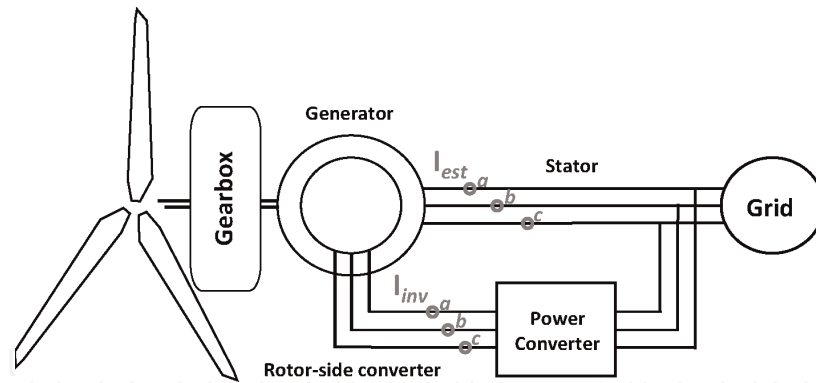
Figure 6.
Drive train diagram with location of sensors in the DFIG.

Sensor location	Label
Stator current phase *a*	I_{est}
Stator current phase *b*	
Stator current phase *c*	
Rotor-side converter current phase *a*	I_{inv}
Rotor-side converter current phase *b*	
Rotor-side converter current phase *c*	

Table 4.
Type of signals used for the analysis.

(in months) and the sampling parameters (sampling rate, in Hertz, and sampling time, in seconds) for each WT DFIG presented in this study.

The data used for the various analyses were extracted from three databases. These comprise currents from sensors located in the induction generator, the stator side and the rotor-side converter, as depicted in **Figure 6**. The electrical measurements used according to **Figure 6** are summarised in **Table 4**.

3.1 Analysis of DFIG1

DFIG1 has two pole pairs, with 1500 rpm rated speed. A test case with the WT operating nearly at full load (825 kW at 1635 rpm) with -0.0915 pu slip was chosen to illustrate the analysis. The negative slip sign is the convention for super-synchronous speed. Under these operating conditions, all possible fault frequencies (as per **Table 2**) were calculated, and peak search and identification were performed in the current spectra, as shown in **Figure 7**.

The supply frequency (50 Hz) and its harmonics (both odd and even) are clearly seen in the spectrum. Another peak naturally present in the spectrum is that corresponding to the difference of the main frequency of the stator and the main frequency of the rotor (f_{s-r} at 54.56 Hz). Then, up to four pairs of f_{FRU} can be seen, as well as the first pair of f_{HRU}. Thus, based on the peaks observed in the spectrum, the presence of rotor electrical unbalance can be concluded.

3.2 Analysis of DFIG2

DFIG2 has three pole pairs, with 1000 rpm rated speed. It presented anomalous vibration levels in the drive-end generator bearing. With only this information, the
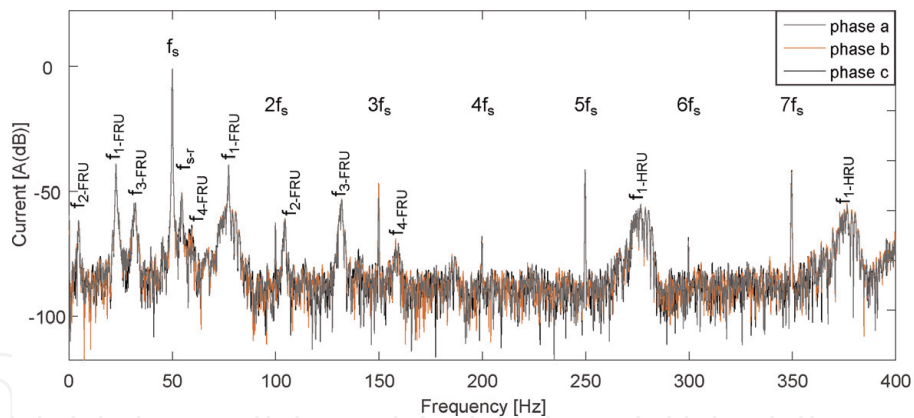
Figure 7.
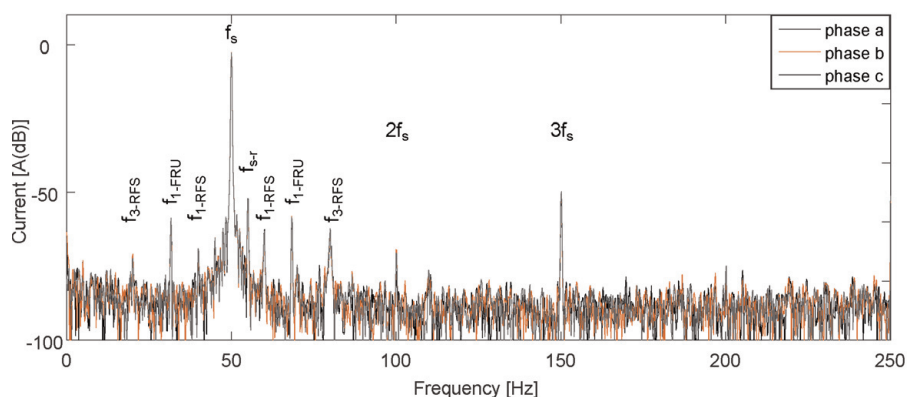*Three-phase current spectra of DFIG1 showing rotor electrical unbalance.*

Figure 8.
Three-phase current spectra of DFIG2 showing rotor mechanical unbalance.

wind farm operator decided to replace the generator bearing. Right after the replacement, the vibration levels decreased. However, a few days later, these levels rose to values similar to those prior to the replacement. Visual inspection of the apparently defective bearing showed no fault in the replaced component, thus, the generator bearing was misdiagnosed.

A measurement with the WT operating at super-synchronous speed (1100 rpm, at 1100 kW power) with -0.01 pu slip was selected for this test case. Once again, the set of potential fault frequencies is calculated, and peak search and identification are carried out on the current spectra, as shown in **Figure 8**.

The supply frequency (f_s) corresponds to the highest peak amplitude (at 50 Hz), as expected. It is odd harmonics are also found (150, 250 Hz, etc.), as well as the difference of the stator and rotor carrier frequencies (f_{s-r}). With regard to fault-related frequency components, no peaks related to bearing fault were found (nor to gearbox either). Only the first pair of f_{FRU} can be identified (thus not fault indicator). Finally, two odd pairs of f_{RFS} are seen, belonging to rotor mechanical asymmetries. The diagnosis achieved was, therefore, rotor unbalance of mechanical nature, i.e. unbalance of the high-speed shaft.

3.3 Analysis of DFIG3

DFIG3 has two pole pairs and 1500 rpm rated speed. It was reported with excessive temperature on the rotor windings. Besides, the generator bearings were replaced two or three times a year. With a 3- to 5-year expected lifetime for these
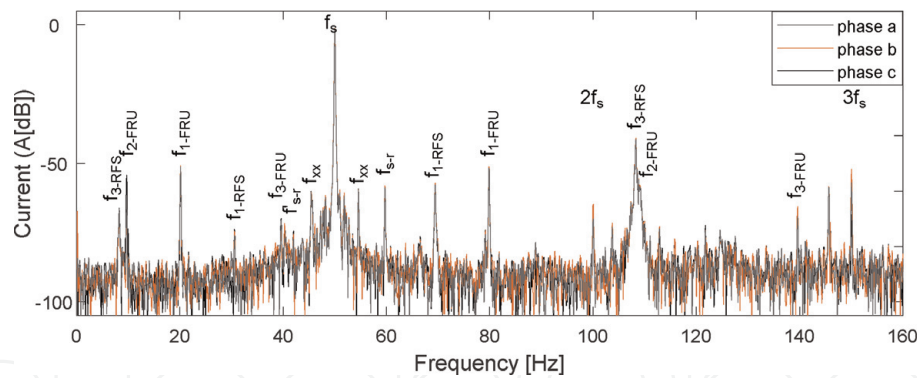
Figure 9.
Three-phase current spectra of DFIG3 showing rotor winding fault.

particular types of generator bearings, the idea that they were suffering damage from a generator fault arose. Thus, CSA was undertaken to find out the health status of the generator.

Similarly to the previous studies, the whole set of potential fault frequency components, as per the formulae previously described, was calculated, and peak search and identification were carried out. To illustrate the analysis, one stationary measurement with the WT operating at 1245 kW and 1791 rpm with per unit slip -0.1941 was selected. Its spectral analysis is shown in **Figure 9**.

Like in the previous analyses, odd and even supply frequency harmonics appear, showing, in this case, certain differences per phase for the second and third harmonics ($2f_s$ and $3f_s$, respectively). Same occurs with the frequency component associated to the difference between the stator carrier frequency (f_s) and the rotor carrier frequency (f_{rotor}), indicated as f_{s-r} in **Figure 9**. Since the measurement was selected with the WT operating at super-synchronous speed, it falls to the right of f_s, as expected. In this case, however, its reflection (denoted as f'_{s-r}) can also be seen to the left of f_s. A minimal amplitude for f'_{s-r} can sometimes be seen; however, the amplitude observed in **Figure 9** for f'_{s-r} on phases a and b is higher than expected. One pair noted as f_{xx} was also found, which does not belong to any of the formulae previously presented.

Regarding fault-related frequency components, three pairs were identified for f_{FRU}. Since more than one pair has been found, it does indicate a mixed eccentricity fault. Finally, two odd pairs of f_{RFS} (f_{1-RFS} and f_{3-RFS}) appear in the current spectra, indicating a fault originating in the rotor. Unlike f_{FRU}, no f_{RFS} pairs are expected to appear in a healthy machine. Hence, it is possible to conclude that DFIG3 has a rotor fault which has led to mixed eccentricity.

4. Conclusions

With the rapid growth of wind energy and development of WTs, researchers and the industry are facing continuous challenges. There is also the fact that the accessibility of offshore wind farms can be limited or restricted for several months. All this, together with the fact that an important share of the existing wind turbine fleet has already achieved its 20-year estimated lifetime, shows that availability and reliability of wind turbines must be developed in parallel. Furthermore, wind energy is expected to play a key role in the short- and long-term electricity market. Thus, the various technical and economical issues surrounding WTs and wind farms must be studied and addressed towards financially viable wind energy.

O&M of wind farms represents an important share of the total expenditure costs; therefore, it is vital to optimise the strategies implemented while increasing reliability and availability of wind turbines. The induction generator is one of the critical components of a WT, together with the drive train and hub and blade assemblies. Under this scenario, the use of electrical measurements to monitor the induction generator has been presented in this chapter.

CSA has been chosen as the CM method for diagnosing three DFIGs of in-service WTs. The technique has been presented, and spectral analyses have been conducted. Fault frequency components related to different faults have been identified in the spectra of the three machines. DFIG1 was diagnosed with rotor electrical unbalance, DFIG2 with rotor mechanical unbalance and DFIG3 with rotor winding fault. CSA has thus been proven as a valid method to diagnose in-service WTs equipped with DFIG that can be implemented in commercial CM systems of WTs.

Acknowledgements

Nomenclature

CBM	condition-based maintenance
CM	condition monitoring
CSA	current signature analysis
DFIG	doubly-fed induction generator
FBM	failure-based maintenance
GWEC	global wind energy council
LCOE	levelized cost of electricity
LTE	lifetime extension
O&M	operation and maintenance
RTU	remaining useful life
SCADA	supervisory control and data acquisition
TBM	time-based maintenance
WT	wind turbine

Author details

Estefania Artigao*, Andrés Honrubia-Escribano, Sergio Martín-Martínez
and Emilio Gómez-Lázaro
Renewable Energy Research Institute and DIEEAC-ETSII-AB, Universidad de
Castilla-La Mancha, Albacete, Spain

*Address all correspondence to: estefania.artigao@uclm.es

IntechOpen

References

[1] Ohlenforst K. Global wind report 2018. Tech. Rep. Global Wind Energy Council; 2019

[2] Honrubia-Escribano A, Gomez-Lazaro E, Fortmann J, Sorensen P, Martin-Martinez S. Generic dynamic wind turbine models for power system stability analysis: A comprehensive review. Renewable and Sustainable Energy Reviews. 2018;**81**(2):1939-1952

[3] Ren G, Liu J, Wan J, Guo Y, Yu D. Overview of wind power intermittency: Impacts, measurements, and mitigation solutions. Applied Energy. 2017;**204**: 47-65

[4] Wang R-J, Gerber S. Magnetically geared wind generator technologies: Opportunities and challenges. Applied Energy. 2014;**136**:817-826

[5] Burt M, Firestone J, Madsen JA, Veron DE, Bowers R. Tall towers, long blades and manifest destiny: The migration of land-based wind from the Great Plains to the thirteen colonies. Applied Energy. 2017;**206**:487-497

[6] Gao C, Sun M, Geng Y, Wu R, Chen W. A bibliometric analysis based review on wind power price. Applied Energy. 2016;**182**:602-612

[7] Ribrant J, Bertling L. Survey of failures in wind power systems with focus on Swedish wind power plants during 1997–2005. In: IEEE Power Engineering Society General Meeting; 2007. pp. 1-8

[8] Spinato F, Tavner PJ, Bussel GJW, Koutoulakos E. Reliability of wind turbine subassemblies. IET Renewable Power Generation. 2008;**3**(4):387-401

[9] Hahn B, Durstewitz M, Rohrig K. Reliability of wind turbines. Journal of Wind Energy. 2007:329-332

[10] de Prada Gil M, Gomis-Bellmunt O, Sumper A. Technical and economic assessment of offshore wind power plants based on variable frequency operation of clusters with a single power converter. Applied Energy. 2014;**125**: 218-229

[11] Koutoulakos E. Wind turbine reliability characteristics and offshore availability assessment [Master's thesis]. Delft, The Netherlands: Delft University, Wind Energy Research Institute; 2010

[12] Reder MD, Gonzalez E, Melero J. Wind turbine failures-tackling current problems in failure data analysis. Journal of Physics: Conference Series. 2016;**753**:072027

[13] Lin Y, Tu L, Liu H, Li W. Fault analysis of wind turbines in China. Renewable and Sustainable Energy Reviews. 2016;**55**:482-490

[14] Carroll J, McDonald A, McMillan D. Failure rate, repair time and unscheduled O&M cost analysis of offshore wind turbines. Wind Energy. 2015;**19**:1107-1119

[15] Wilson G, McMillan D. Assessing wind farm reliability using weather dependent failure rates. Journal of Physics: Conference Series. 2014;**524**(1): 012181

[16] Hines VA, Ogilvie AB, Bond CR. Continuous reliability enhancement for wind (CREW) database: Wind plant reliability benchmark. Tech. Rep. Sandia National Laboratories, Albuquerque, New Mexico/Livermore, California; 2013

[17] Dinwoodie FQ, McMillan D. Analysis of offshore wind turbine operation and maintenance using a novel time domain meteo-ocean

modelling approach. In: ASME Turbo Expo 2012: Turbine Technical Conference and Exposition. American Society of Mechanical Engineers; 2012

[18] Wilkinson M, Harman K, Hendriks B, Spinato F, van Delft T, Garrad G, et al. Measuring wind turbine reliability—Results of the Reliawind project. In: European Wind Energy Association Conference; 2011. pp. 1-8

[19] Stenberg A, Holttinen H. Analysing failure statistics of wind turbines in Finland. In: European Wind Energy Conference; 2010

[20] Tavner PJ, Xiang J, Spinato F. Reliability analysis for wind turbines. Wind Energy. 2007;**10**:1-18

[21] Sinha Y, Steel J. A progressive study into offshore wind farm maintenance optimisation using risk based failure analysis. Renewable and Sustainable Energy Reviews. 2015;**42**:735-742

[22] Blanco MI. The economics of wind energy. Renewable and Sustainable Energy Reviews. 2009;**13**(6):1372-1382

[23] Fischer K, Besnard F, Bertling L. Reliability-centered maintenance for wind turbines based on statistical analysis and practical experience. IEEE Transactions on Energy Conversion. 2012;**27**(1):184-195

[24] Márquez FPG, Tobias AM, Pérez JMP, Papaelias M. Condition monitoring of wind turbines: Techniques and methods. Renewable Energy. 2012;**46**:169-178

[25] Qiao W, Zhang P, Chow M-Y. Condition monitoring, diagnosis, prognosis, and health management for wind energy conversion systems. IEEE Transactions on Industrial Electronics. 2015;**62**(10):6533-6535

[26] Tian Z, Jin T, Wu B, Ding F. Condition based maintenance optimization for wind power generation systems under continuous monitoring. Renewable Energy. 2011;**36**(5): 1502-1509

[27] Bussel GJW, Zaaijer MB. Reliability, availability and maintenance aspects of large-scale offshore wind farms, a concepts study. In: MAREC 2011: Proceedings of the 2-Day International Conference on Marine Renewable Energies (Institute of Marine Engineers Edition); 2001

[28] Lu B, Li Y, Wu X, Yang Z. A review of recent advances in wind turbine condition monitoring and fault diagnosis. In: IEEE Power Electronics and Machines in Wind Applications (PEMWA); 2009. pp. 1-7

[29] Sheng S. Improving component reliability through performance and condition monitoring data analysis. Tech. Rep. Wind Farm Data Management & Analysis North America; 2015

[30] McMillan D, Ault GW. Towards quantification of condition monitoring benefit for wind turbine generators. In: European Wind Energy Conference Exhibition; Milan, Italy; 2007

[31] Jardine AKS, Lin D, Banjevic D. A review on machinery diagnostics and prognostics implementing condition-based maintenance. Mechanical Systems and Signal Processing. 2006;**20**: 1483-1510

[32] Yam R, Tse P, Li L, Tu P. Intelligent predictive decision support system for condition-based maintenance. The International Journal of Advanced Manufacturing Technology. 2001;**17**(5): 383-391

[33] Nilsson J, Bertling L. Maintenance management of wind power systems

using condition monitoring systems—Life cycle cost analysis for two case studies. IEEE Transactions on Energy Conversion. 2007;**22**(1):223-229

[34] Qiao W, Lu D. A survey on wind turbine condition monitoring and fault diagnosis—Part II: Signals and signal processing methods. IEEE Transactions on Industrial Electronics. 2015;**62**(10): 6546-6557

[35] Hameed Z, Hong Y, Cho Y, Ahn S, Song C. Condition monitoring and fault detection of wind turbines and related algorithms: A review. Renewable and Sustainable Energy Reviews. 2009; **13**(1):1-39

[36] Qiao W, Lu D. A survey on wind turbine condition monitoring and fault diagnosis—Part I: Components and subsystems. IEEE Transactions on Industrial Electronics. 2015;**62**(10): 6536-6545

[37] Kabir MJ, Oo AM, Rabbani N. A brief review on offshore wind turbine fault detection and recent development in condition monitoring based maintenance system. In: IEEE Power Engineering Conference AUPEC; 2015. pp. 1-7

[38] Coronado D, Fischer K. Condition monitoring of wind turbines: State of the art, user experience and recommendations. Tech. Rep. Fraunhofer Institute for Wind Energy and Energy System Technology IWES Northwest; 2015

[39] Yang W, Tavner PJ, Crabtree C, Feng Y, Qiu Y. Wind turbine condition monitoring: Technical and commercial challenges. Wind Energy. 2012;**17**(5): 673-693

[40] Maldonado J, Alvarez O. A review of concepts and methods for wind turbines condition monitoring. In: IEEE Computer and Information Technology (WCCIT), 2013 World Congress; 2014

[41] Amirat Y, Benbouzid MEH, Al-Ahmar E, Bensaker B, Turri S. A brief status on condition monitoring and fault diagnosis in wind energy conversion systems. Renewable and Sustainable Energy Reviews. 2009;**13**(9):2629-2636

[42] Popa LM, Jensen B-B, Ritchie E, Boldea I. Condition monitoring of wind generators. In: IEEE Industry Applications Conference, 38th IAS Annual Meeting; 2003. pp. 1839-1846

[43] Singh GK, Kazzaz S. Induction machine drive condition monitoring and diagnostic research—A survey. Electric Power Systems Research. 2003;**64**(2): 145-158

[44] Tautz-Weinert J, Watson SJ. Using SCADA data for wind turbine condition monitoring—A review. IET Renewable Power Generation. 2016;**11**(4):382-394

[45] Gonzalez E, Tautz-Weinert J, Melero J, Watson SJ. Statistical evaluation of SCADA data for wind turbine condition monitoring and farm assessment. Journal of Physics: Conference Series. 2018;**1037**:032038

[46] Warner E. Global Wind Report. Annual market update. Tech. Rep. Global Wind Energy Council; 2015

[47] Rubert T, McMillan D, Niewczas P. A decision support tool to assist with lifetime extension of wind turbines. Renewable Energy. 2017;**120**(1):423-433

[48] Ziegler L, Gonzalez E, Rubert T, Smolka U, Melero JJ. Lifetime extension of onshore wind turbines: A review covering Germany, Spain, Denmark, and the UK. Renewable and Sustainable Energy Reviews. 2017;**82**:1261-1271

[49] Tavner PJ. Review of condition monitoring of rotating electrical machines. IET Electric Power Applications. 2007;**2**(4):215-247

[50] Benbouzid MEH. A review of induction motors signature analysis as a medium for faults detection. IEEE Transactions on Industrial Electronics. 2000;**47**(5):984-993

[51] Siddique A, Yadava G, Singh B. A review of stator fault monitoring techniques of induction motors. IEEE Transactions on Energy Conversion. 2005;**20**(1):106-114

[52] Benbouzid MEH, Kliman GB. What stator current processing-based technique to use for induction motor rotor faults diagnosis? IEEE Transactions on Energy Conversion. 2003;**18**(2):238-244

[53] Mohanty A, Kar C. Fault detection in a multistage gearbox by demodulation of motor current waveform. IEEE Transactions on Industrial Electronics. 2006;**53**(4): 1285-1297

[54] Blodt M, Granjon P, Raison B, Rostaing G. Models for bearing damage detection in induction motors using stator current monitoring. IEEE Transactions on Industrial Electronics. 2008;**55**(4):1813-1822

[55] Shahriar MR, Borghesani P, Tan AC. Electrical signature analysis-based detection of external bearing faults in electromechanical drivetrains. IEEE Transactions on Industrial Electronics. 2018;**65**(7):5941-5950

[56] Alewine K, Chen W. A review of electrical winding failures in wind turbine generators. IEEE Electrical Insulation Magazine. 2012; **28**(4):8-13

[57] Yazidi A, Henao H, Capolino G, Artioli M, Filippetti F, Casadei D. Flux signature analysis: An alternative method for the fault diagnosis of induction machines. In: IEEE Powertech; 2005. pp. 1-6

[58] Artigao E, Honrubia-Escribano A, Gomez-Lazaro E. Current signature analysis to monitor DFIG wind turbine generators: A case study. Renewable Energy. 2018;**116**:5-14

[59] Artigao E, Koukoura S, Honrubia-Escribano A, Carroll J, McDonald A, Gómez-Lázaro E. Current signature and vibration analyses to diagnose an in-service wind turbine drive train. Energies. 2018;**11**(4):960

[60] Cheng F, Qu L, Qiao W, Wei C, Hao L. Fault diagnosis of wind turbine gearboxes based on DFIG stator current envelope analysis. IEEE Transactions on Sustainable Energy. 2018;**10**:1044

[61] Siau J, Graff A, Soong W, Ertugrul N. Broken bar detection in induction motors using current and flux spectral analysis. Australian Journal of Electrical and Electronics Engineering. 2004;**1**(3):171-178

[62] Acosta G, Verucchi C, Gelso E. A current monitoring system for diagnosing electrical failures in induction motors. Mechanical Systems and Signal Processing. 2006;**20**(4): 953-965

[63] Siddiqui KM, Giri VK. Broken rotor bar fault detection in induction motors using transient current analysis. International Journal of Electronics and Communication Technology. 2011;**2**(4): 114-119

[64] Nandi S, Toliyat HA, Li X. Condition monitoring and fault diagnosis of electrical motors—A review. IEEE Transactions on Energy Conversion. 2005;**20**(4):719-729

[65] Bellini A, Filippetti F, Franceschini G, Tassoni C. Quantitative evaluation of induction motor broken bars by means of electrical signature analysis. IEEE Transactions on Industry Applications. 2001;**37**(5):1248-1255

[66] Kliman GB, Koegl RA, Stein J, Endicott RD, Madden MW. Noninvasive detection of broken rotor bars in operating induction motors. IEEE Transactions on Energy Conversion. 1988;**3**(4):873-879

[67] Rodriguez PVJ, Negrea M, Arkkio A. A simplified scheme for induction motor condition monitoring. Mechanical Systems and Signal Processing. 2008;**22**(5):1216-1236

[68] JJung JH, Lee JJ, Kwon BH. Online diagnosis of induction motors using MCSA. IEEE Transactions on Industrial Electronics. 2006;**53**(6):1842-1852

[69] Kliman GB, Stein J. Methods of motor current signature analysis. Electric Machines and Power Systems. 1992;**20**(5):463-474

[70] Joksimovic GM. The detection of inter-turn short circuits in the stator windings of operating motors. IEEE Transactions on Industrial Electronics. 2000;**47**(5):1078-1084

[71] Douglas H, Pillay P, Barendse P. The detection of interturn stator faults in doubly-fed induction generators. In: Fourtieth IAS Annual Meeting. Conference Record of the 2005 Industry Applications Conference; 2005. pp. 1097-1102

[72] Mehala N. Condition monitoring and fault diagnosis of induction motor using motor current signature analysis [PhD thesis]. Kurukshetra, India: National Institute of Technology, Kurukshetra; 2010. Registration No. 2K07-NITK-PhD-1160-E

[73] Thomson WT, Fenger M. Current signature analysis to detect induction motor faults. IEEE Industry Applications Magazine. 2001;**7**(4):26-34

[74] Thomson WT, Gilmore RJ. Motor current signature analysis to detect faults in induction motor drives—

Fundamentals, data interpretation and industrial case histories. In: Proceedings of the Thirty-Second Turbomachinery Symposium; 2003

[75] Rajagopalan S, Habetler TG, Harley RG, Sebastian T, Lequesne B. Current/voltage-based detection of faults in gears coupled to electric motors. IEEE Transactions on Industry Applications. 2006;**42**(6):1412-1420

[76] Kia SH, Henao H, Capolino G-A. Gearbox monitoring using induction machine stator current analysis. In: IEEE International Symposium on Diagnostics for Electric Machines, Power Electronics and Drives (SDEMPED). IEEE; 2007. pp. 149-154

[77] Kia SH, Henao H, Capolino G-A. Gear tooth surface damage fault detection using induction machine electrical signature analysis. In: 9th IEEE International Symposium on Diagnostics for Electric Machines, Power Electronics and Drives (SDEMPED). IEEE; 2013. pp. 358-364

[78] Kar C, Mohanty AR. Monitoring gear vibrations through motor current signature analysis and wavelet transform. Mechanical Systems and Signal Processing. 2006;**20**:158-187

[79] Cheng F, Qu L, Qiao W. Fault prognosis and remaining useful life prediction of wind turbine gearboxes using current signal analysis. IEEE Transactions on Sustainable Energy. 2017;**9**:157

[80] Neti P, Zhang P, Shah M, Younsi K. Electrical signature analysis based online monitoring of drive-trains for doubly-fed wind generators. In: 38th Annual Conference on IEEE Industrial Electronics Society (IECON); 2012

[81] Faiz J, Moosavi S. Eccentricity fault detection—From induction machines to DFIG—A review. Renewable and

Sustainable Energy Reviews. 2016;**55**: 169-179

[82] Gritli Y, Stefani A, Rossi C, Filippetti F, Chatti A. Experimental validation of doubly fed induction machine electrical faults diagnosis under time-varying conditions. Electric Power Systems Research. 2011;**81**(3): 751-766

[83] Gritli Y, Zarri L, Rossi C, Filippetti F, Capolino G-A, Casadei D. Advanced diagnosis of electrical faults in wound-rotor induction machines. IEEE Transactions on Industrial Electronics. 2013;**60**(9):4012-4024

[84] Bellini A, Filippetti F, Tassoni C, Capolino G-A. Advances in diagnostic techniques for induction machines. IEEE Transactions on Industrial Electronics. 2008;**55**(12):4109-4126

[85] Djurovic S, Williamson S, Renfrew A. Dynamic model for doubly-fed induction generators with unbalanced excitation, both with and without winding faults. IET Electric Power Applications. 2009;**3**(3):171-177

[86] Williamson S, Djurovic S. Origins of stator current spectra in DFIGs with winding faults and excitation asymmetries. In: IEEE International Electric Machines and Drives Conference, IEMDC'09; Vol. 9; 2009. pp. 563-570